Materials Transactions, Vol. 54, No. 10 (2013) pp. 1894 to 1897
©2013 The Japan Institute of Metals and Materials

Effect of Shot Peening on Surface Characteristics of Ni-Based Single-Crystal Superalloy

YanHua Chen[1,2] and ChuanHai Jiang[1,*]

[1]*School of Materials Science and Engineering, Shanghai Jiao Tong University, No. 800 Dongchuan Road, Shanghai, 200240, P. R. China*
[2]*School of Physical Science and Technology, Xinjiang University, Urumqi, 830046, P. R. China*

The effect of shot peening on surface characteristics of DD3 Ni-based single-crystal superalloy including microstructures, texture and residual stress were investigated, utilizing XRD analysis. Results showed that the polycrystals was introduced into the surface of single-crystal specimen by shot peeing and the initial texture (200) was erased after 60 s-processing. The variation in microstructure was mainly influenced by the processing time and finer domains as well higher microstrain were obtained after 60 s-processing. The value of residual stress depended upon processing time and measurement direction. In the early period of processing (~10 s), residual stress was anisotropy, being significant smaller in ⟨110⟩ direction. With the processing time increased, the anisotropic residual stress gradually changed to isotropic residual stress, due to domain-orientation randomization, domain refinement and increase in plastic strain. Also increasing processing time could significantly enhance the magnitude of residual stress and the microhardness. In addition, the influence of processing time on work hardening and residual stress was discussed, based on the deformation mechanism. [doi:10.2320/matertrans.M2013153]

(Received April 22, 2013; Accepted July 16, 2013; Published September 25, 2013)

Keywords: *microstructure, residual stress, X-ray diffraction, shot peening, nickel-based single-crystal superalloy*

1. Introduction

Nickel-based single-crystal superalloys have been widely used for the turbine section of the aircraft engine, because of the high reliability.[1)] However, in the process of manufacturing, the surface is treated mechanically and which inevitably introduces residual stresses into the surface of component.[1)] Generally, these stresses are tensile and which promote crack initiation/propagation and lead to a reduction in fatigue strength.[2)] Therefore, in order to improve the fatigue strength, the crack initiation and propagation in the surface must be suppressed using mechanical surface treatment. As an effective surface treatment method, shot peening (SP) has been widely used in aerospace, automotive and power generation industries, due to the introduction of favorable compressive residual stresses (CRS) and deeper work hardening zone into the surface of component.[3–6)] This process has been adopted to improve the fatigue life of polycrystalline nickel-base superalloy components.[7–9)] However, at present, few reports have been available to describe the effect of shot peening on the single-crystal Ni-based superalloys.

The objective of this work is to study the effect of shot peening on surface characteristics of DD3 Ni-based single-crystal superalloy using XRD analysis, including microstructures, texture and residual stress. Also microhardness at different processing time was measured. In addition, the deformation mechanism and the effect of processing time on work hardening and compressive residual stress based on the strengthening mechanism were discussed.

2. Experimental

The material used in this work is DD3 Ni-based single-crystal superalloy with a nominal chemical composition of 9.5 chromium, 5.9 aluminum, 2.2 titanium, 5.2 wolfram, 5 cobalt, 3.8 molybdenum, and balance nickel, in weight percent. The heat treatment regimes of the superalloys are given as follows: 1250°C × 4 h, AC (air cooling) +870°C × 32 h, AC. After the crystal orientation was determined by Laue back reflection, the specimens were machined from cast bars, with their longitudinal axes parallel to the [001]-orientation, with a square cross-section (10 mm × 10 mm) and a parallel length of 3 mm. The deviations from the ideal orientation were less than 7°. Before SP, the specimens were polished electrolytically. SP time is 10, 30, 60 and 120 s, respectively.

The SP treatment was performed on an air blast machine (Carthing Machinery Company, China). Shot media was Al_2O_3 ceramic beads, with average diameter of 0.3 mm. The jet pressure was about 0.3 Mpa and the Almen intensity was 0.13 mmA. Hardness measurements were conducted on a digital microhardness tester (DHV-1000, China) with an applied load of 0.49 N. The distance between two successive indentations was set at least ten times the impression sizes to avoid any interference between adjacent indentations, and each hardness value reported here was the average of ten readings. The X-ray diffraction patterns were collected on Rigaku Ultima IV X-ray diffractometer, which operated at 40 kV/40 mA with Cu-$K\alpha$ radiation ($\lambda = 0.154056$ nm). Besides, Div H. L. Slit, Div Slit, Sct Slit and Receiving Slit were fixed as 10 mm, 0.5°, 0.5° and 0.15 mm respectively. The residual stresses were obtained by X-ray Stress Analyzer (LXRD, Proto, Canada) with Mn-$K\alpha$ radiation, using the {311}-plane. A Young's modulus of $E = 115$ GPa and Poisson's ratio of $\nu = 0.3$ was used to calculate the residual stresses from the observed lattice strains, not considering the elastic anisotropy. The range of tilting angles (ψ) is 0–45°, and the range of azimuthal angle (φ) is 0–180°, with an interval of 15°.

3. Results and Discussion

X-ray diffraction (XRD) profile is mainly determined by the microstructure of the material, and can be influenced by

*Corresponding author, E-mail: ch_jiang2013@163.com

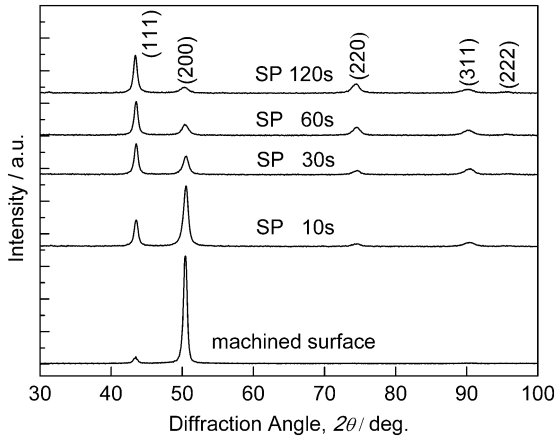

Fig. 1 XRD patterns of the DD3 single-crystal superalloy before and after shot peening (10, 30, 60 and 120 s).

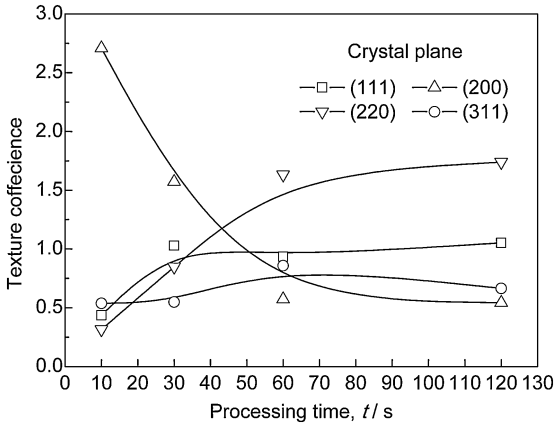

Fig. 2 Variation of texture coefficient in (111), (200), (220) and (311) crystal planes with processing time.

the existing of texture which could change the relative intensities of the diffraction peaks. Figure 1 shows the evolution of the X-ray diffraction patterns with the processing time, and all the characteristic peaks of samples have been indexed. It can be seen that, after 10 s-processing, all the characteristic peaks of crystalline nickel have been discerned, a clear indicative of the generation of polycrystals at the surface region. When increasing the processing time to 60 s, an obvious decrease in intensity of (200) peak and increase in intensities of (111) and (220) peak are found. And after 120 s-processing, only a slight variation in intensities is discerned. These finds indicate that the initial texture (200) is weakened and which reaches a plateau beyond 60 s-processing.

In order to quantify this phenomenon, the texture coefficient has been calculated and shown in Fig. 2. A texture coefficient (*TC*) using the Harris method was adopted to observe the relative degree of preferred orientation among crystal planes as follows;[10)]

$$TC_{(hkl)} = \frac{I_{(hkl)}/I_{0(hkl)}}{\frac{1}{N}\sum(I_{(hkl)}/I_{0(hkl)})} \quad (1)$$

where, $I_{(hkl)}$, $I_{0(hkl)}$ and N are the measured integrated intensities of the specimen, the standard integrated intensities of Ni powder and the number of reflections, respectively.

It can be seen from Fig. 2 that, *TC* in (200) crystal plane of 10 s-processed specimen is about 2.7 and smaller than that of un-peened specimen (~4.0), implying the weakening of initial orientation by SP. However, *TC* in (200) crystal plane is much larger than that in other three crystal plane, a clear indication of both the existence of strong texture and the preferred orientation being still along the (200) crystal plane after 10 s-processing. When increasing processing time to 60 s, an obvious decrease in $TC^{(200)}$ and a significant increase in $TC^{(220)}$ are noticed, together with a slight increase in $TC^{(111)}$ and $TC^{(311)}$. On this condition, the maximum *TC* (~1.6) appears in (220) crystal plane and larger than $TC^{(200)}$ (~0.6), suggesting the elimination of initial texture (200) and the generation of deformation texture (220). When further increasing processing time to 120 s, no obvious change is found in *TC* of the four crystal planes, implying the improvement on the texture stability.

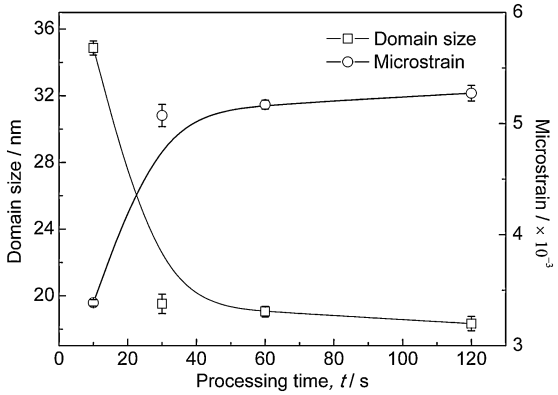

Fig. 3 Variations of domain size and microstrain in (200) peaks of specimens processed for 10, 30, 60 and 120 s.

This phenomenon is mainly attributed to the random deformation direction at and near surface. SP is in fact a process of repeated deformation. For each deformation, distribution of the plastic flow direction is random, which results in the random deformation direction. Hence, the initial texture is weakened distinctly after SP. On the other hand, during further deformation, the domains with random orientation are arranged gradually along a certain direction, which results in a new preferred orientation distribution. For fcc crystals, the main plane texture is {110} after deformation, which is consistent with our studies.

Besides, an obvious broadening in (200) diffraction peak is noticed with the processing time prolonged, indicative of the domain refinement and the increase in microstrain. Via *Materials Analysis Using Diffraction* (*MAUD*), the variations in domain size and microstrain of (200) peak have been quantified and shown in Fig. 3. The *MAUD* software, recently developed whole pattern fitting *Rietveld* software, can perform a simultaneous refinement of both material structure and microstructure described through the measure of lattice parameters, crystallite size and microstrain.[11)] From Fig. 3, a significant decrease in domain size and increase in microstrain can be observed in (200) peak after SP till 60 s-processing and the changes become unconspicuous beyond 60 s-processing. This reveals that the microstructure is

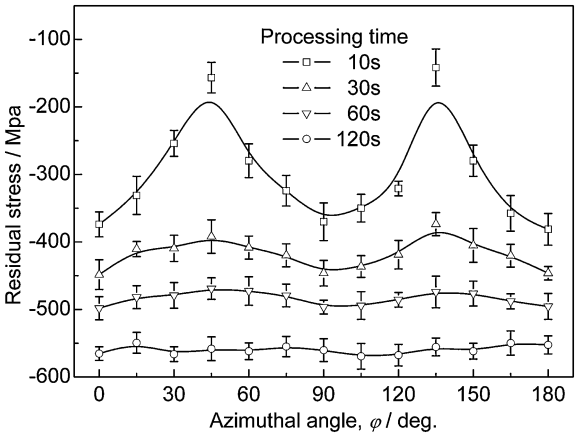

Fig. 4 Distributions of the surface compressive residual stress of specimens processed for 10, 30, 60 and 120 s.

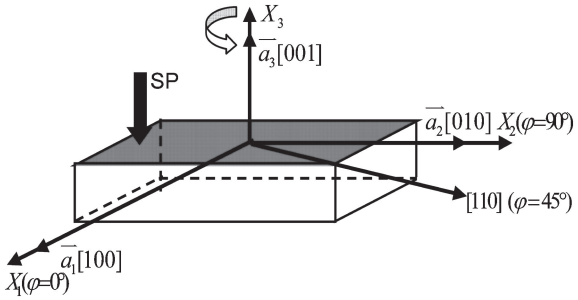

Fig. 5 Schematic diagram of shot peening and measurement, where a_i denotes the crystal coordinate system and X_i refers to the specimen coordinate system.

improved after SP, especially significant after 60 s-processing or more, due to the finer domain and higher microstrain.

According to the Hall-Petch relation ($\sigma_s = \sigma_0 + KD^{-1/2}$, where σ_s is the yield strength of material, D is domain size, σ_0 and K are constants), finer domains lead to an improvement on yield strength.[12] On the other hand, in deformed metals, microstrain mainly comes from dislocations because not only they are always the main defects, but also they are the major components or can play an important role in other defects.[13,14] Therefore, the variation trend of microstrain is similar to that of dislocation density. According to Baily-Hirsch equation[15] ($\sigma_s = \sigma_0 + \beta\mu b\rho^{1/2}$, where σ_s is the strength of material, ρ is the dislocation density, σ_0 is the intrinsic strength of annealed material, β is a correction factor specific to the material, μ is the shear modulus and b is the magnitude of the Burgers vector), the metals exhibit high strength if there is larger number of dislocations. Therefore, better mechanical properties can be obtained in the specimens processed with 60 s or more, due to the finer domains and higher microstrain/density dislocations.

Considering the anisotropic properties of the Ni-based single-crystal alloys, the residual stresses at different measurement directions (φ angles) were measured after SP and depicted in Fig. 4. It can be seen that, CRS has been introduced into the surface after 10 s-processing. On this condition, one interesting phenomenon should be noticed that the surface compressive residual stress (SCRS) varies with the measurement directions and shows wavy distribution. Figure 5 shows the geometrical relationship of measurement directions and crystal direction. According to Figs. 4 and 5, it reveals that the maximum SCRS appears along the ⟨100⟩ directions ($\varphi = 0$, 90 and 180°), while the minimum SCRS emerges along the ⟨110⟩ directions ($\varphi = 45$ and 135°). The deviation between the $SCRS^{max}$ and $SCRS^{min}$ is very large, with a value of 230 Mpa, which indicates that the CRS in the surface is high anisotropic. When increasing the processing time to 30 s, the SCRS increases rapidly. Evidently, the increment of SCRS at different measurement directions is different. Compared the value of SCRS at different measurement directions, it can be noted that, the biggest increment occurs in the ⟨110⟩ directions ($\varphi = 45$ and 135°), while the smallest increment appears in the ⟨100⟩ directions ($\varphi = 0$, 90 and 180°). The deviation between $SCRS^{max}$ and $SCRS^{min}$ is about 75 Mpa and much smaller than that in 10 s-processed specimen, which reveals that the anisotropy of SCRS is reduced significantly after 30 s-processing. With the processing time further prolonged, the SCRS increases progressively and the deviation between $SCRS^{max}$ and $SCRS^{min}$ decreases gradually. When increasing processing time to 120 s, there is only a slight difference in the values of SCRS at different measurement directions, a clear indication of uniform distribution of CRS in the surface.

These phenomena can be explained by the deformation mechanism of single crystal and polycrystals. In the process of SP, great deals of shot balls impacting on the surface from different directions, which causes elastic and plastic deformation at and near surface of the single-crystal specimen.[3–6] The deformation in single crystal is mainly produced by the dislocation slip at room temperature. For face centered cubic (fcc) crystal, the primary slip systems is in {111} plane with ⟨110⟩ direction. Therefore, dislocations slip mainly along the ⟨110⟩ directions in the process of SP, which leads to a smaller CRS value.[16] As the processing time increases, so does the magnitude of deformation. Larger deformation induces the domain refinement and rotation, which leads to the generation of finer polycrystals and domain-orientation randomization at the shot-peened surface. The increase in domain-orientation randomization will lead to the decrease in the anisotropy of SCRS. Moreover, finer domains can significantly enhance deformation uniformity and reduce the stress concentration.[17,18] Therefore, with the processing time prolonged, the anisotropic residual stress gradually changes to equi-biaxial residual stress. On the other hand, the plastic deformation is anisotropic in the process of SP. During repeated bumping, the plastic strains gradually increases and becomes saturated in each direction, which also leads to the SCRS distribution tending to be isotropic.

Also, the Vickers microhardness of specimens before and after SP have been measured and shown in Fig. 6. It can be seen that SP can improve the hardness of the surfaces and the improvement is no longer significant beyond 60 s-processing. The values of microhardness are influenced by the microstructure and stress state, which is determined by the domain size, the amount of microstrain and the magnitude of SCRS. Therefore, the increments of hardness with the processing time are mainly due to the finer domains, higher value of microstrain and SCRS. Since the tensile strength is closely proportional to the hardness ($HV \cong 3\sigma_b$; where HV is the

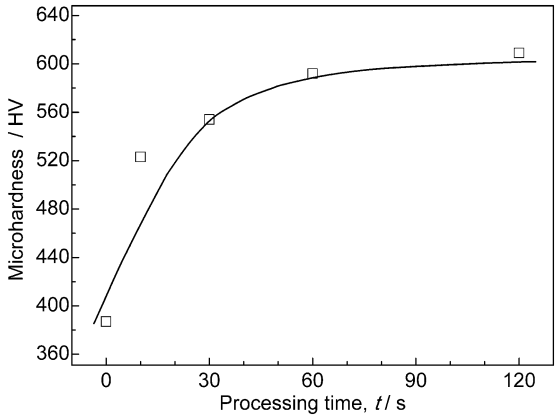

Fig. 6 Variations of microhardness of specimens before and after shot peening (10, 30, 60 and 120 s).

Vickers hardness and σ_b is the tensile strength).[19] Thereupon, larger the Vickers microhardness is, higher the tensile strength is. Therefore, the tensile strength is enhanced after SP and especially significant after 60 s-processing or more, indicative of an improvement on fatigue performance at and near surface.

4. Conclusion

Benefits due to shot peening are increase in resistance to fatigue, which mainly is determined by the microstructure and compressive residual stress in the surface. According to the discussion above, it reveals that SP can erase the initial texture of the Ni-based single-crystal superalloy and produce a nano-polycrystalline shot-peened surface. Microstructure, residual stress and microhardness in the surface can be improved after SP and especially significant after 60 s- and 120 s-processing, due to the finer domain, higher microstrain, stable microstructure, uniform stress distribution, greater SCRS and larger microhardness at the shot-peened surface, all of which are beneficial for improving the fatigue properties. Considering that there is no significant improvement in microstructure, stress state and microhardness beyond 60 s-processing, 60 s-proceesing is optimal in this work.

Acknowledgement

Financial support from the National Natural Science Foundation of China under the project No. 50771066 is acknowledged.

REFERENCES

1) T. M. Pollock and S. Tin: J. Propul. Power. **22** (2006) 361–374.
2) M. E. Fitzpatrick, P. J. Withers, A. Baczmanski, M. T. Hutchings, R. Levy, M. Ceretti and A. Lodini: Acta Mater. **50** (2002) 1031–1040.
3) B. X. Feng, X. N. Mao, G. J. Yang, L. L. Yu and X. D. Wu: Mater. Sci. Eng. A **512** (2009) 105–108.
4) Q. Feng, C. H. Jiang and Z. Xu: Mater. Des. **47** (2013) 68–73.
5) W. Z. Luan, C. H. Jiang and V. Ji: Mater. Trans. **50** (2009) 837–840.
6) W. Z. Luan, C. H. Jiang and V. Ji: Mater. Trans. **50** (2009) 1499–1501.
7) J. W. Tian, K. Dai, J. C. Villegas, L. Shaw, D. L. Klarstrom and A. L. Ortiz: Mater. Sci. Eng. A **493** (2008) 176–183.
8) L. A. Ortiz, J. W. Tian, L. L. Shaw and P. K. Liaw: Scr. Mater. **62** (2010) 129–132.
9) W. Österle, P. X. Li and G. Nolze: Mater. Sci. Eng. A **262** (1999) 308–311.
10) C. S. Barrett and T. B. Massalaski: *Structure of Metals*, 3rd revised ed., (Pergamon Press, New York, 1980) pp. 204–208.
11) L. Lutterotti, P. Scardi and P. Maistrelli: J. Appl. Crystallogr. **25** (1992) 459–462.
12) M. A. Meyers, A. Mishra and D. J. Benson: Progress Mater. Sci. **51** (2006) 427–556.
13) T. Ungár: Mater. Sci. Eng. A **309–310** (2001) 14–22.
14) T. Ungár: Scr. Mater. **51** (2004) 777–781.
15) R. S. Liu and J. Y. Li: Mater. Sci. Eng. A **114** (1989) 127–132.
16) Y.-H. Chen, C.-H. Jiang, Z. Wang and K. Zhan: Powder Diffr. **25** (2010) 355–358.
17) G. A. Salishchev and S. Y. Mironov: Russ. Phys. J. **44** (2001) 596–601.
18) R. A. Masumura, P. M. Hazzledine and C. S. Pande: Acta Mater. **46** (1998) 4527–4534.
19) Y. J. Kwon, I. Shigematsu and N. Saito: Scr. Mater. **49** (2003) 785.